Journal of Power Sources 242 (2013) 171–178

Contents lists available at SciVerse ScienceDirect

Journal of Power Sources

journal homepage: www.elsevier.com/locate/jpowsour

Hierarchical shuttle-like Li_2FeSiO_4 as a highly efficient cathode material for lithium-ion batteries

Jinlong Yang, Xiaochun Kang, Daping He, Tao Peng, Lin Hu, Shichun Mu*

State Key Laboratory of Advanced Technology for Materials Synthesis and Processing, Wuhan University of Technology, Wuhan 430070, China

HIGHLIGHTS

- A hierarchical shuttle-like Li_2FeSiO_4 was synthesized using hydrothermal method.
- The growth mechanism of the shuttle-like Li_2FeSiO_4 was discussed.
- The shuttle-like Li_2FeSiO_4 possessed excellent electrochemical performance.

ARTICLE INFO

Article history:
Received 11 March 2013
Received in revised form
14 May 2013
Accepted 20 May 2013
Available online 28 May 2013

Keywords:
Electrode
Shuttle-like
Cathode materials
Lithium-ion battery

ABSTRACT

We successfully synthesized the novel hierarchical shuttle-like Li_2FeSiO_4 using one step hydrothermal method with ethylene glycol assisted. The growth mechanism of the shuttle-like Li_2FeSiO_4 constructed of nanosingle crystals was discussed and its electrochemical performance as a cathode material for lithium ion battery was investigated. Astonishingly, the 1st discharge specific capacity of the new material without carbon coating was 180.6 mA h g^{-1} at 0.1 C with a remarkably high Coulombic efficiency of 97.5%, and an improved high-rate capability (71.0 mA h g^{-1} at 2 C) was offered which is comparable to the commonly carbon-coated Li_2FeSiO_4. Moreover, it exhibited a very stable discharge specific capacity at current densities from 0.1 to 2 C. Its excellent electrochemical performance can be ascribed to the significantly improved diffusion coefficient of lithium ions ($5.6421 * 10^{-11}$ cm^2 s^{-1}), which was greatly larger than the reported carbon-coated Li_2FeSiO_4 nanocomposites and diatomic metallic ions (Ni^{2+}, Cu^{2+}, Zn^{2+}) doped Li_2FeSiO_4. These indicate the shuttle-like Li_2FeSiO_4 is a very promising cathode material for lithium-ion batteries.

1. Introduction

Lithium iron silicate (Li_2FeSiO_4) first reported by Nytén et al. [1] possesses excellent chemical stability and safety imparted by the covalently bonded SiO_4 groups [2,3], nontoxic, and inexpensive materials (Fe and Si are abundant in the earth) with a high reversible capacity (potential capacity of 332 mAh g^{-1}) [4–10]. However, the slow lithium-ion diffusion rate (approximately $1 * 10^{-14}$ cm^2 s^{-1}) [11,12] and low electronic conductivity [6,13] of Li_2FeSiO_4 lead to a low rate capability which becomes one of the biggest obstacles to commercial applications. Numerous approaches have been investigated to circumvent this main issue by ameliorating the intrinsic and extrinsic properties of bulk Li_2FeSiO_4, including porous nanostructure designing [14], particle size reduction [15], supervalent or isovalent cation doping in crystals [16–18], typical carbon coating or fabrication of carbonaceous matrices [14,19], and introduction of conductive inorganic compounds [13] or organic polymers [10].

Recently, hierarchical architectures and materials from nano- to micro-scale building blocks have attracted more and more attention in electrode materials studies for lithium ion battery, due to their noticeable advantages such as unique size, special morphologies, large surface area, high tap density and better physical–chemical properties. The hierarchical architectures constructed of nano-scale single-crystal blocks also have been confirmed to greatly enhance lithium and electron transfer rates, in favor of improving electrochemical performance as cathodes. These architectures include dumbbell-like, sheaf-fagot, spindle-like, flower-like, and nano-plates lithium iron phosphate (LFP) materials [20–24], which present high capacity, high-rate and good cyclic performance.

We report here for the first time the novel hierarchical shuttle-like architecture of Li_2FeSiO_4 which is expected to have a high lithium-ion diffusion rate as cathode materials for lithium ion

* Corresponding author.
E-mail addresses: msc@whut.edu.cn, mushichun@gmail.com (S. Mu).

0378-7753/$ – see front matter © 2013 Elsevier B.V. All rights reserved.
http://dx.doi.org/10.1016/j.jpowsour.2013.05.088

batteries. Up to now, various methods have been developed to prepare Li_2FeSiO_4, including solid-state reaction [1,25], sol–gel [13,26], hydrothermal [13,27], spray technology [28], supercritical fluid [10], microwave-solvothermal [15], combustion [29] and sol–gel-assisted hydrothermal syntheses [12]. Among them, the hydrothermal method offers mild synthesis conditions, high degree of crystallinity and narrow particle size distribution of products. Extraordinarily, architecture electrode materials with specific morphologies from nano-scale building blocks could be easily obtained via hydrothermal method. However, almost no researches related to the Li_2FeSiO_4 cathode materials with hierarchical architectures have been concerned. Therefore, in this work, ethylene glycol was used as auxiliary to prepare the hierarchical shuttle-like Li_2FeSiO_4 architecture via one step hydrothermal synthesis. Moreover, its formation mechanism and electrochemical performance for lithium battery cathode materials were investigated.

2. Experimental

2.1. Material synthesis

All chemicals used were analytical grade (purchased from the Sinopharm Chemical Reagent Co., Ltd), and employed directly without any purification. Firstly, 0.0125 mol of $Fe(Ac)_2 \cdot 4H_2O$ was thoroughly dissolved in 20 mL ethylene glycol, and then 40 mL deionized water solution with 0.0125 mol of TEOS and 0.05 mol of $LiOH \cdot 2H_2O$ was rapidly added. Under vigorous stirring for about 10 min, the mixture was transferred into 100 mL of Teflon-lined stainless steel autoclave and maintained at 180 °C for 8 days. After reaction, the resultant grayish-black precipitation was collected, washed by water and ethanol for several times, and dried at 80 °C in vacuum for 12 h. To investigate the formation process of the shuttle-like Li_2FeSiO_4 architecture, parallel experiments were conducted by keeping all the parameters constant and only changing the hydrothermal reaction temperature and time.

2.2. Characterization

X-ray diffraction (XRD) measurement was performed to investigate the crystallographic information using a D8 Advance X-ray diffractometer with a non-monochromated Cu Kα X-ray source. Field-emission scanning electron microscopy images were collected with a Hitachi S-4800 at an acceleration voltage of 10 kV. Transmission electron microscopy and high-resolution transmission electron microscopy images were recorded with a JEM-2100 F STEM/EDS microscope.

Electrochemical coin cells were assembled inside an argon-filled dry-box with lithium metal anodes, Celgard™ 2400 as separators and 1 mol L^{-1} LiPF6 in EC:DMC:EMC (1:1:1 by volume) as electrolytes. The cathode electrode was made of active materials, carbon black and poly (vinylidene fluoride) binders in a weight ratio of 75:15:10. The components were previously mixed as viscous slurry in *N*-methyl-2-pyrrolidone solvent, and coated uniformly on aluminum foil, and then dried at 120 °C for at least 6 h in vacuum. The typical active material loading was 2.0 mg cm^{-2}. Galvanostatic charge/discharge measurement was performed in the potential range from 1.5 to 4.8 V vs. Li/Li^+ with a multichannel battery testing system (LAND CT2001A). Cyclic voltammetry was tested with an electrochemical workstation (CHI 604D).

3. Results and discussion

SEM images of the Li_2FeSiO_4 synthesized via one-step ethylene glycol assisted hydrothermal method at 180 °C for 8 days are shown

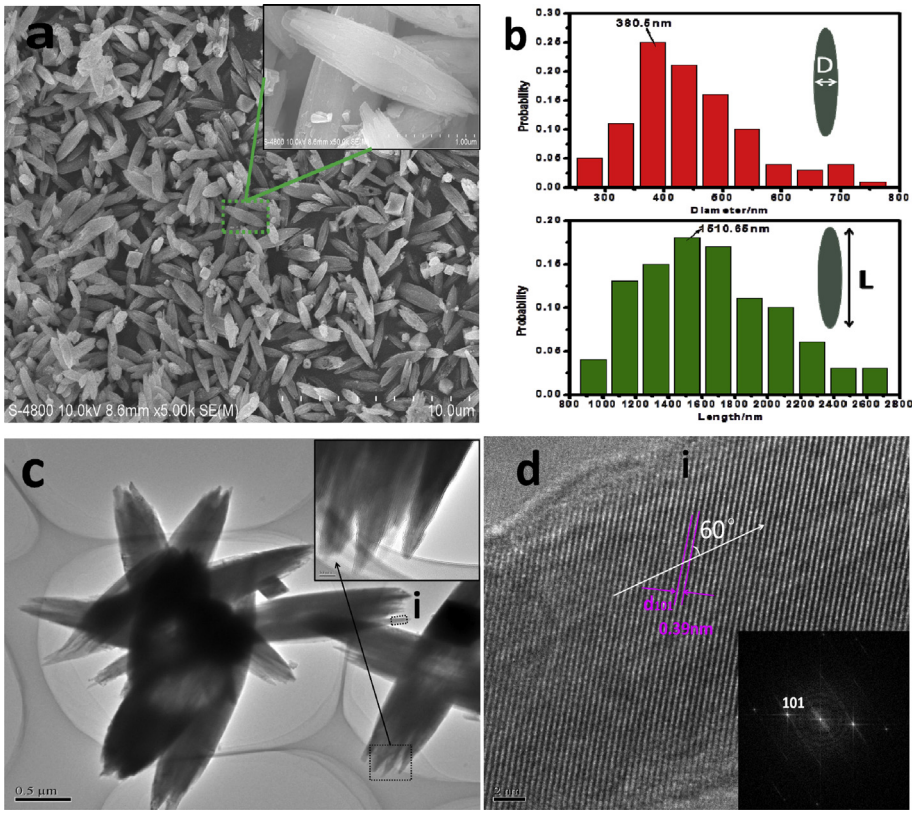

Fig. 1. Images of (a) SEM, (b) the length and diameter distributions, (c) TEM and (d) HRTEM (the inset is the corresponding FFT pattern) of samples obtained at 180 °C for 8 days.

in Fig. 1a. The monodispersed shuttles were obtained, which have smooth surfaces with ~1.5 um in mean particle length and ~380 nm in diameter (Fig. 1b). The clearer shuttle-like architecture can be depicted from the inset of Fig. 1a and the TEM micrograph in Fig. 1c. The shuttles have a small void space at the tips (the inset of Fig. 1c) which is likely due to the gaps of the smaller nanoscale crystals; this indicates that the shuttles are assembled with a large amount of nano-crystals. This unique structure can promote the accessing of electrolyte to active material surface and shortening of lithium-ion diffusion distances, which would improve the electrochemical properties.

Fig. 1d shows a high-resolution TEM (HR-TEM) micrograph taken from the selected area in Fig. 1c, and the inset, corresponding to Fast-Fourier-Transform (FFT) pattern of the HRTEM image, displays a single-crystalline pattern with sharp diffraction spots. The measured fringe spacing values are 0.39 nm which corresponds to (101) planes of orthorhombic Li_2FeSiO_4. This result proves that the primary nano-crystals are well crystallized with pure orthorhombic Li_2FeSiO_4 phase, and the crystal growth orientation inclines to (101) planes at an angle of 60°.

A typical XRD pattern of the shuttle-like Li_2FeSiO_4 is shown in Fig. 2. The distinguished sharp intense peaks correspond to the highly crystalline nature of the as-prepared Li_2FeSiO_4. As it was reported, there are at least three different structures for Li_2FeSiO_4, namely the orthorhombic (S.G. $Pmn2_1$) [30], monoclinic (S.G. $P2_1/n$) [3] and orthorhombic (S.G. Pmnb) [31] structures. The diffraction peaks of the shuttle-like Li_2FeSiO_4 were indexed according to the orthorhombic structure (S.G. $Pmn2_1$), and the lattice parameters ($a = 0.628183$ nm, $b = 0.533348$ nm, and $c = 0.497258$ nm) were obtained, which are consistent with the previous report [30]. Few impurities like Fe_3O_4 were also unavoidably present in samples due to a hydrothermal process [13,22]. The crystallite size calculated using Jade 6.5 software from the most intense peaks in Fig. 2 is 31.8 nm, which also provides strong evidence that the shuttle-like Li_2FeSiO_4 was assembled with smaller nanostructural Li_2FeSiO_4 crystals. The $Pmn2_1$ structure can be viewed along the *a*-axis in the inset of Fig. 2 where the lithium-ion can be embedded and emerged along the broken line in the *b*-axis direction with the current flowing through [32].

To understand the growth mechanism of hierarchical shuttle-like Li_2FeSiO_4 architectures, the influences of hydrothermal conditions including reaction temperature from 150 to 200 °C and time up to eight days on the structures and morphologies of the products were investigated. Different morphologies of the samples obtained with hydrothermal temperatures are shown in Fig. 3. After hydrothermal reaction at 150 °C for 8 days, the Li_2FeSiO_4 had an incomplete shuttle-like structure. As the temperature increased to 180 °C,

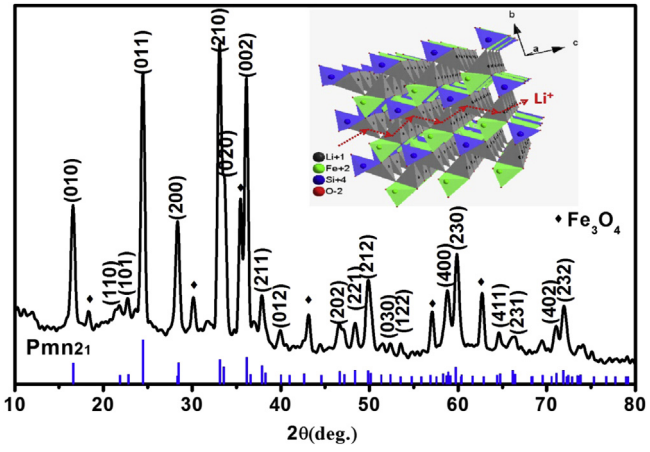

Fig. 2. XRD patterns of shuttle-like Li_2FeSiO_4 obtained at 180 °C for 8 days.

a perfect and novel shuttle-like Li_2FeSiO_4 with approximately 1.5 um in length and 380 nm in diameter was offered. However, when the temperature was up to 200 °C, the shuttle grew thicker, and the aspect ratio was approximately 600 nm to 2 um. These results show that the hydrothermal reaction temperature had a significant influence on the morphology of Li_2FeSiO_4. XRD patterns (Fig. 3) of all samples present that the phases were closely matched with the $Pmn2_1$ space group Li_2FeSiO_4. In addition, the whole peaks intensities were enhanced with increase of the reaction temperature; this shows that the hydrothermal temperature played a great role in formation of high crystallinity shuttle-like Li_2FeSiO_4. However, an appropriate hydrothermal temperature (180 °C) can be chosen to synthesize perfect shuttle-like Li_2FeSiO_4 with larger aspect ratio. As can be seen in Fig. 4, at the same hydrothermal temperature (180 °C), the morphologies of samples were irregular after 12 h reaction, and the phases were mainly composed of amorphous substance accompanying small amount of Fe_3O_4 crystals by XRD analyses (Fig. 4). After aging up to one day, most of spherical particles emerged in the samples, the peaks of XRD patterns correspond to the phases of Li_2SiO_3 and Fe_3O_4, respectively. When the reaction time increased to three days, the samples were spherical particles coated by nano-crystals corresponding to orthorhombic structure Li_2FeSiO_4. If the time was further prolonged to six days, all samples consisted of short crystalline Li_2FeSiO_4. After two days the perfect shuttle-like structure Li_2FeSiO_4 was present.

Based on the above results, a possible formation of the hierarchical shuttle-like Li_2FeSiO_4 can be proposed, which is schematically illustrated in Fig. 5. The proposed mechanism includes the following sequential reaction (from steps (1)–(3)). First of all, the mixture of water, ethylene glycol, Fe $(CH_3COO)_2 \cdot 4H_2O$, TEOS and $LiOH \cdot 2H_2O$ rapidly turns to dark-green ferrous hydroxide colloidal particles (step (1)). During 12 h hydrothermal reaction, with the aid of the OH^- catalyzed reaction, TEOS hydrolyzes and subsequently cross-link to a $(SiO_2)_x$ colloid network (Fig. 5a, top) by reaction

$$x\mathrm{Si}(\mathrm{OC_2H_5})_4 + 2x\mathrm{H_2O} \rightarrow (\mathrm{SiO_2})_x + 4x\mathrm{C_2H_5OH} \quad (1)$$

where ions (Li^+, CH_3COO^-, OH^-), molecules (H_2O, EG, C_2H_5OH) and ferrous hydroxide colloid are embedded. Meanwhile, with reaction, Li_2SiO_3 can be obtained by reaction of Li^+ and OH^- with cross-linked $(SiO_2)_x$ (step (2))

$$2x\mathrm{Li^+} + 2x\mathrm{OH^-} + (\mathrm{SiO_2})_x \rightarrow x\mathrm{Li_2SiO_3} + x\mathrm{H_2O} \quad (2)$$

Then the condensed form of micro-spherical particles together with trapped ferrous hydroxide colloids would be developed as shown in Fig. 5b (top). As the reaction time increases to three days, the micro-spherical particles start to be dissolved and many short crystalline Li_2FeSiO_4 forms on the surface (Fig. 5c, top) by reaction (step (3))

$$\mathrm{Fe(OH)_2} + \mathrm{Li_2SiO_3} \rightarrow \mathrm{Li_2FeSiO_4} + \mathrm{H_2O} \quad (3)$$

Ethylene glycol, with hydrophilic oxygen atoms and much higher viscosity [33] (21 mPa s, 20 °C) than water ($1.0087 * 10^{-3}$ mPa s, 20 °C), easily adheres to surfaces of Li_2FeSiO_4 particles and reacts to obtained nanocrystalline Li_2FeSiO_4 under hydrothermal condition. With the increase of the amount and size of nano-crystals, the micro-spherical particle thoroughly collapses on the sixth day (Fig. 5d, top). Two days later the short crystals further grow into micro shuttles (Fig. 5e, top). The corresponding morphologies of samples prepared at different hydrothermal treatment stages are shown from SEM images in the range of a to e at the bottom of Fig. 5.

The typical charge–discharge curves of the hierarchical shuttle-like Li_2FeSiO_4 obtained at 180 °C for 8 days in different

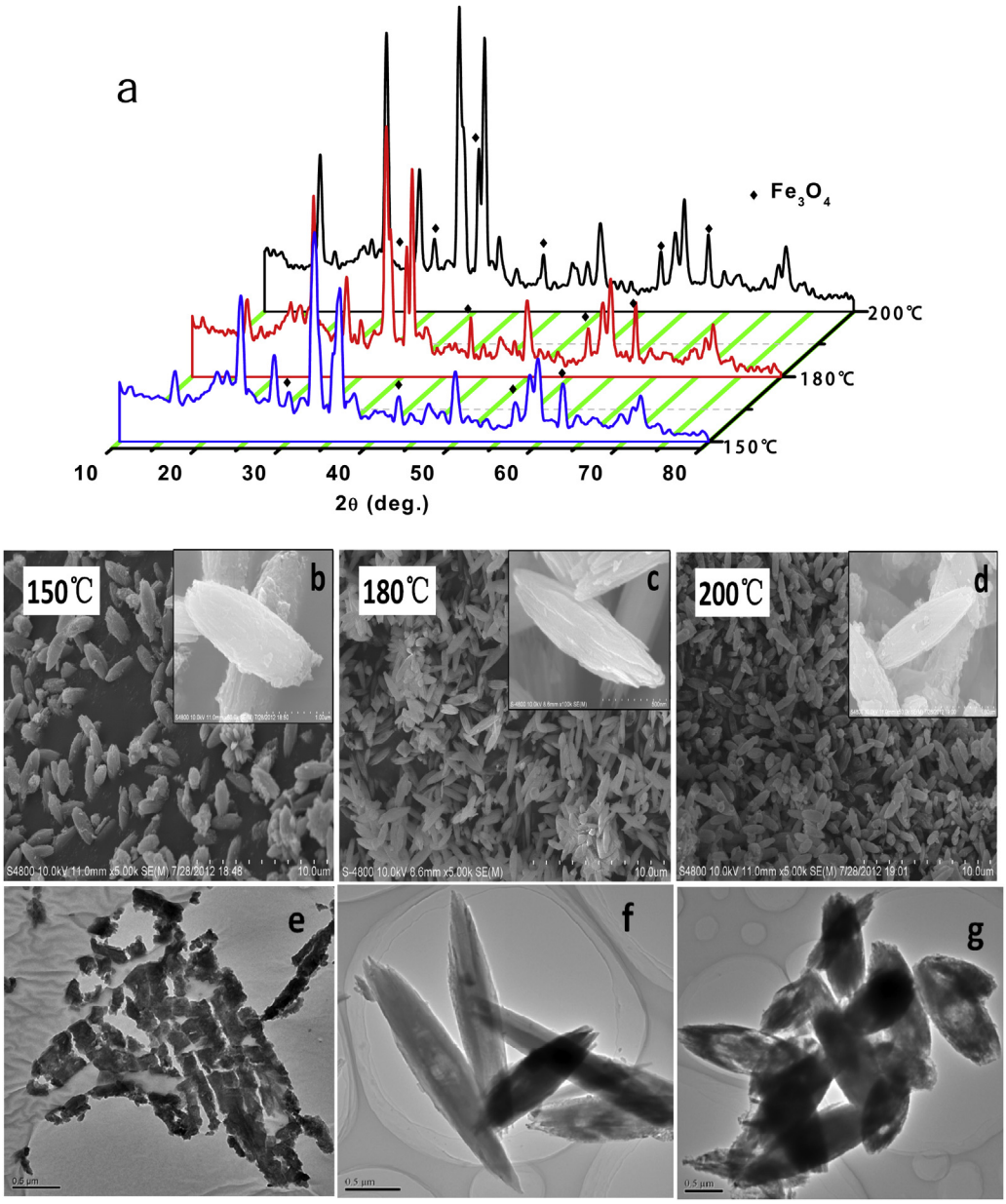

Fig. 3. X-ray diffraction patterns (a), scanning electron microscopy images (b–d) and transmission electron microscopy (e–g) of the shuttle-like Li_2FeSiO_4 architectures obtained at 150 °C, 180 °C, and 200 °C.

cycles with a current density of 0.1 C between 1.5 and 4.8 V are shown in Fig. 6a. The 1st discharge specific capacity of shuttle-like Li_2FeSiO_4 was up to 180.6 mA h g^{-1} with a high Coulombic efficiency of 97.5%. Subsequently, the 2nd discharge specific capacity decreased to 160.2 mA h g^{-1}, and the charge curve was largely different from that of the 1st cycle, which shows an irreversible capacity loss. With charge–discharge cycle tests, the specific capacity maintained at above 150.0 mA h g^{-1} in 20 cycles. To investigate the charge–discharge principle of the shuttle-like Li_2FeSiO_4, dQ/dV vs. voltage plots of the charge–discharge curves of the shuttles at a current density of 0.1 C between 1.5 and 4.8 V are given (Fig. 6b). The initial charge peaks at higher voltages of approximately 4.5 and 4.3 V, and the discharge peaks at lower voltages of about 2.85, 2.6 and 1.82 V, correspond to the potential plateau in the charge–discharge curves, respectively. It can be observed that after the 2nd cycle, these potential plateaus apart from that at 2.6 V disappeared, whereas a new charge potential plateau at approximately 3.15 V occurred. The charge plateau voltage at about 4.5 V dropped off the curve might be ascribed to the extraction of O (Li_2O) as a result of oxidation of oxide ion [34], and the disappearance of voltage plateaus at approximately 4.3, 2.85 and 1.82 V could be attributed to the structural rearrangement during the first electrochemical cycling [1]. On the subsequent cycles the charge potential plateau at approximately 3.15 V shifted toward lower potential (approximately 2.95 V), and the discharge potential plateau at about 2.85 V gradually became shorter and disappeared in the end, which could be caused by the electrochemical polarization and a small contribution of the changes of structures when the current passed through the electrode. After three cycles, the rearrangement of the structure was completely over, which exhibited better stability for the shuttle-like Li_2FeSiO_4.

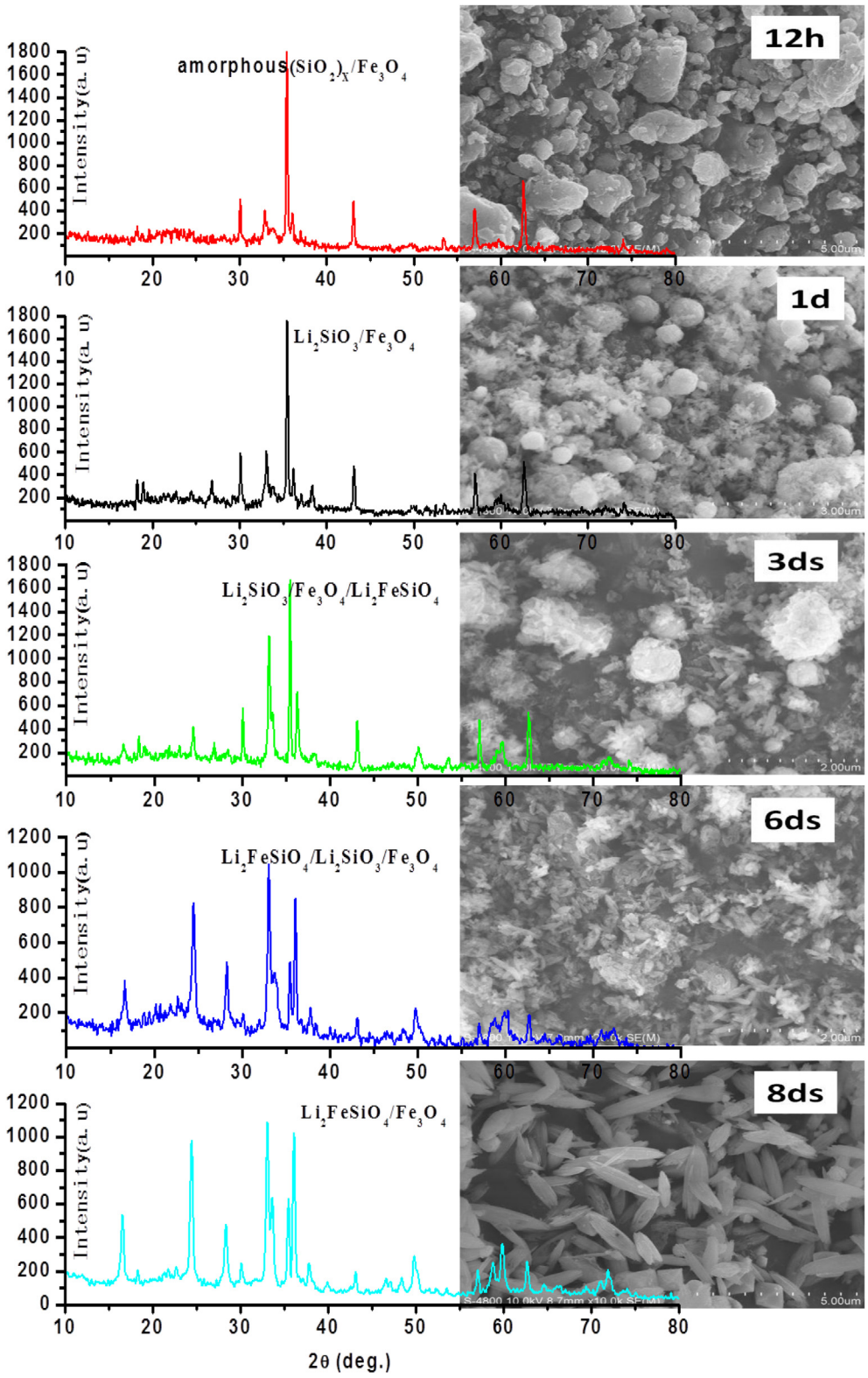

Fig. 4. Phase and morphologies of the samples with different hydrothermal time.

The hierarchical shuttle-like Li_2FeSiO_4 electrode was performed at different C-rates. The typical charge–discharge curves under various current densities (1 C = 166 mA g^{-1}) are present in Fig. 6c. At a low rate of 0.1 C, the shuttle-like Li_2FeSiO_4 electrode delivered wider plateau at about 3 V. With increment of C-rate from 0.1 to 2 C, the plateau was shortened, and the charge specific capacities under different current density of 0.2, 0.5, 1 and 2 C were 159.4, 127.3, 82.0 and 71.0 mA h g^{-1}, respectively, which correspond to 136.4, 111.8, 78.6 and 67.8 mA h g^{-1} for the discharge specific capacities. The results are in good agreement with that of commonly reported

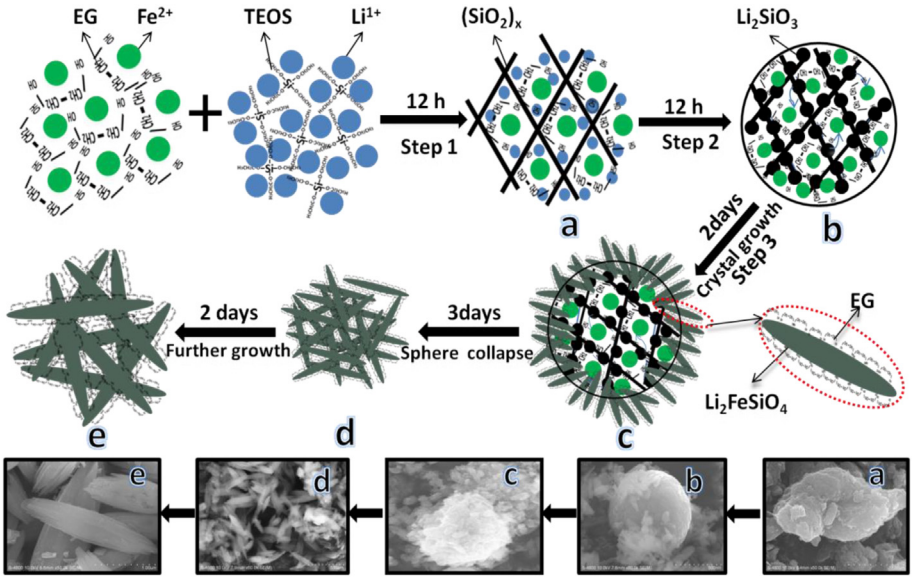

Fig. 5. Schematic of formation for the hierarchical shuttle-like Li_2FeSiO_4.

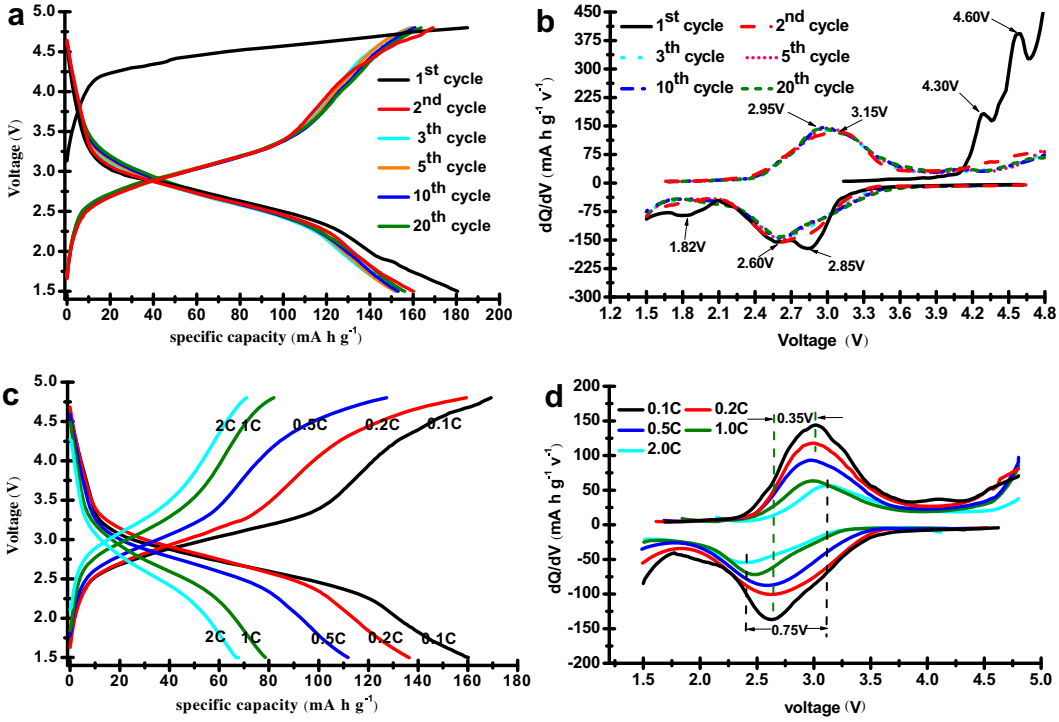

Fig. 6. Electrochemical performances of the shuttle-like Li_2FeSiO_4 obtained at 180 °C for 8 days. (a) Typical charge–discharge curves and (b) d*Q*/d*V* vs. voltage plots of the charge–discharge curves at 0.1 C (1 C = 166 mA g^{-1}), (c) the rate charge–discharge curves and (d) d*Q*/d*V* vs. voltage plots of the charge–discharge curves of shuttle-like Li_2FeSiO_4 under various current densities.

carbon-coated Li_2FeSiO_4 [35,36]. The d*Q*/d*V* vs. voltage plots of charge–discharge curves under various current densities are shown in Fig. 6d, it can be seen that the potential of lithium-ion embedded and disembedded shifted at variational current densities. As a low current (0.1 C) passed the hierarchical shuttle-like Li_2FeSiO_4 electrodes, the distance between the charge peaks and discharge peaks was 0.35 V, and widened along with the current enhancement (up to 0.75 V at 2 C), which was more than two times of that at 0.1 C.

The cyclic performance of the hierarchical shuttle-like Li_2FeSiO_4 at different current densities is shown in Fig. 7. It was found that the hierarchical shuttle-like Li_2FeSiO_4 electrodes exhibited a very stable discharge capacity with almost no discernible capacity decay at different current densities from 0.1 to 2 C rates after the initial 3 cycles due to the rearrangement of the structure. Subsequently, comparing with the samples obtained under different hydrothermal conditions and/or maintained time, the hierarchical shuttle-like Li_2FeSiO_4 architectures obtained at 180 °C for eight days had

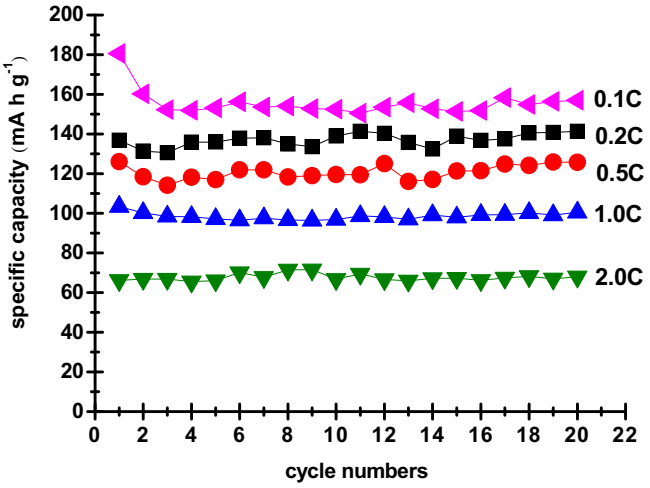

Fig. 7. Initial 20 cyclic properties of shuttle-like Li_2FeSiO_4 under various current densities.

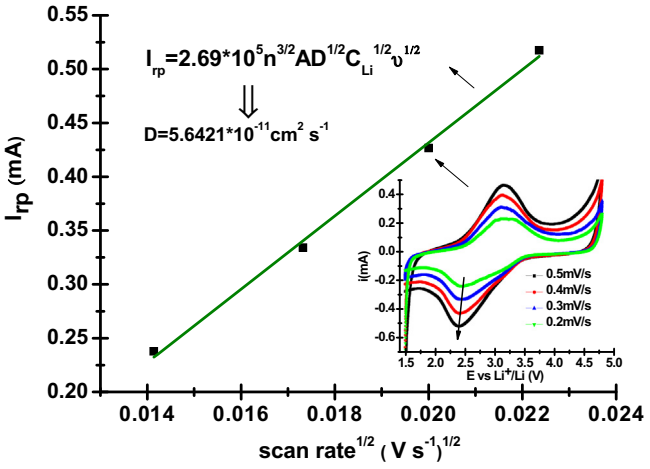

Fig. 9. Lithium-ion diffusion calculation for the shuttle-like Li_2FeSiO_4 achieved at 180 °C for 8 days, the inset shows the formula and cyclic voltammetry curves at different scan rates.

a higher capacity and much better cycle property at a relatively high current density of 0.5 C (Fig. 8). These results indicate that the nude shuttle-like Li_2FeSiO_4 has great electrochemical properties as cathode materials for lithium-ion batteries.

In order to well understand the effect of the hierarchical shuttle-like Li_2FeSiO_4 architectures on the excellent electrochemical performance of electrodes, the diffusion coefficient of lithium ions (D_{Li}) was calculated from a linear relationship between peak current Irp (A) and the square root of the scan rate $\upsilon^{1/2}$ $(V\ s^{-1})^{1/2}$, according to the equation [14,37] from Fig. 9 inset, where n is the number of electrons per reaction species, A is the electrode area (1.13 cm^2 in this study), and C_{Li} is the bulk concentration of the lithium ion in the electrode (0.040 mol cm^{-3} for Li_2FeSiO_4). A good liner relationship between Ip and $\upsilon^{1/2}$ from the cyclic voltammetry curves at different scan rates can be offered, and the determined D_{Li} is 5.6421 * 10^{-11} cm^2 s^{-1}, which is larger than the previous carbon-coated nanocomposites [14] and diatomic metallic ions (Ni^{2+}, Cu^{2+}, Zn^{2+}) doped [16] Li_2FeSiO_4. Therefore, we believe that the excellent electrochemical performance of our Li_2FeSiO_4 could be mainly contributed to the much better lithium-ion diffusion rate which depends on the unique morphology, architecture and the suitable crystal size of the shuttle-like Li_2FeSiO_4.

From the charge curves, the structure changed during the first electrochemical cycle. As shown in Fig. S1, the XRD peaks of the cycled sample were almost the same as that of the original one, except of the loss of the Li_2SiO_3 impurity peaks. However, very minor changes of the lattice constant (Table S1) took place in further analyses, including that the length of both *a*- and *b*-axis in

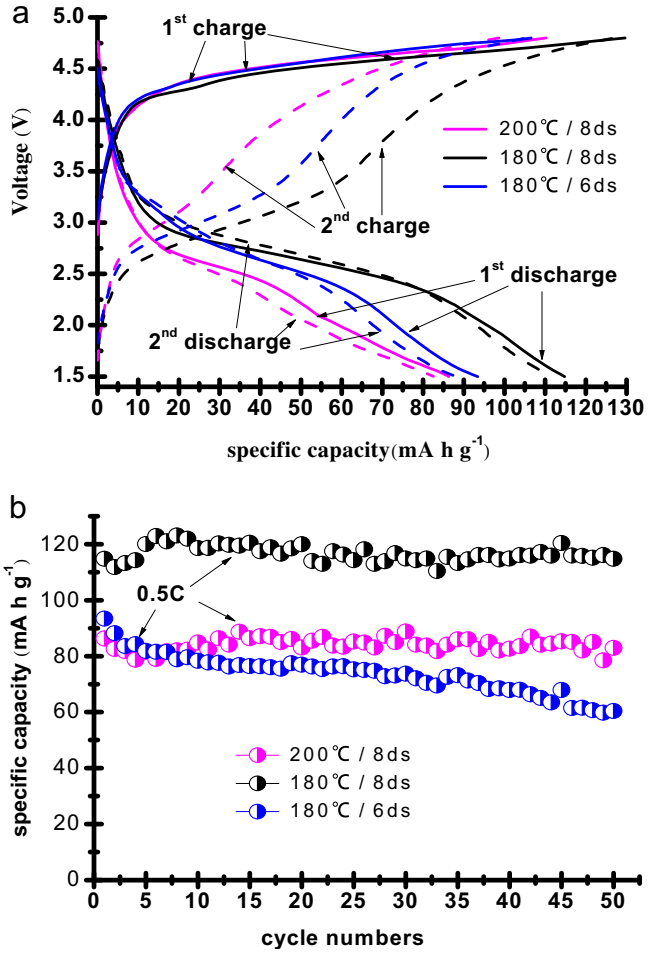

Fig. 8. Charge–discharge curves (a) and cycle performances (b) of different samples at a relatively high current rate of 0.5 C.

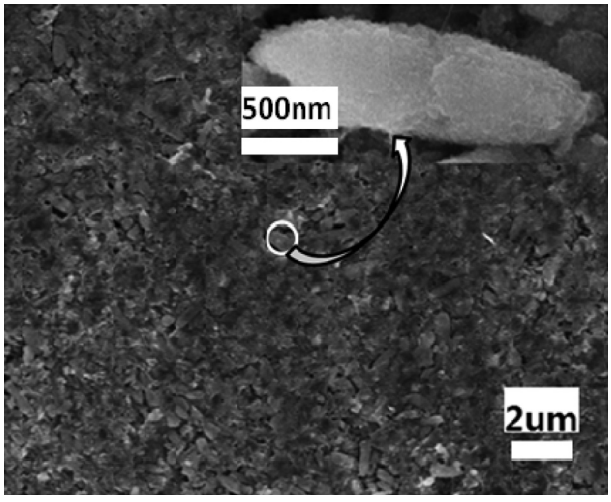

Fig. 10. SEM images of the sample after the 1st cycle.

the cycle sample became short except of *c*-axis. As reported by Arroyo-de Dompablo et al. [2], the *c*-axis increases is the elongate Fe–Fe and Fe–Si distances caused by the Si–O–Fe angles open (get closer to 180°), and the *a*- and *b*-axis decreases is attributed to the shortening of the Fe–O and Si–Si distances, respectively. Nytén et al. [38] further confirmed this structure change is some local interchange of the Li ions (in the 4b site) due to the delithiated during the 1st charge, as well as showed that this cycling structure possesses better stability than that before cycling. More importantly, the SEM images in Fig. 10 show that the new electrode material after the 1st cycle almost possessed original morphology and dispersity. This indicates that the structural change was very weak and had no intrinsic effect on the stability of the shuttle-like Li_2FeSiO_4 in crystal structure, morphology as well as dispersity, which ensured its subsequent stable cyclic performance.

4. Conclusions

The shuttle-like Li_2FeSiO_4 was synthesized via one step hydrothermal method. The shuttle had a hierarchical assembly architecture consisting of a large amount of nano-crystals from SEM, HRTEM and XRD techniques. This new Li_2FeSiO_4 performed high reversible capacity (159.4 mA h g^{-1} at 0.1 C, 115.0 mA h g^{-1} at 0.5 C, and 71.0 mA h g^{-1} at 2 C), high coulombic efficiency in the first cycle, and significantly enhanced cycling performance and C-rate capability as cathode materials for lithium-ion batteries. The great improvement of the electrochemical performance for the shuttle-like Li_2FeSiO_4 without carbon coating could be caused by the greatly improved lithium-ion diffusion rate of its unique hierarchical architecture. We believe that the new hierarchical shuttle-like Li_2FeSiO_4 material is very promising to make the next generation of high-energy-density lithium-ion batteries.

Acknowledgments

This research was financially supported by the National Science Foundation of China (No. 50972112).

Appendix A. Supplementary information

Supplementary data related to this article can be found online at http://dx.doi.org/10.1016/j.jpowsour.2013.05.088.

References

[1] A. Nytén, A. Abouimrane, M. Armand, T. Gustafsson, J.O. Thomas, Electrochem. Commun. 7 (2005) 156–160.
[2] M.E. Arroyo-de Dompablo, M. Armand, J.M. Tarascon, U. Amador, Electrochem. Commun. 8 (2006) 1292–1298.
[3] S. Nishimura, S. Hayase, R. Kanno, M. Yashima, N. Nakayama, A. Yamada, J. Am. Chem. Soc. 130 (2008) 13212–13213.
[4] D.P. Lv, W. Wen, X.K. Huang, J.Y. Bai, J.X. Mi, S.Q. Wu, Y. Yang, J. Mater. Chem. 21 (2011) 9506–9512.
[5] Z. Chen, S. Qiu, Y. Cao, Ji. Qian, X. Ai, K. Xie, X. Hong, H. Yang, J. Mater. Chem. A (2013), http://dx.doi.org/10.1039/C3TA00611E.
[6] R. Dominko, J. Power Sources 184 (2008) 462–468.
[7] M.S. Islam, R. Dominko, C. Masquelier, C. Sirisopanaporn, A.R. Armstrong, P.G. Bruce, J. Mater. Chem. 21 (2011) 9811–9818.
[8] C. Sirisopanaporn, C. Masquelier, P.G. Bruce, A.R. Armstrong, R. Dominko, J. Am. Chem. Soc. 133 (2011) 1263–1266.
[9] P. Larsson, R. Ahuja, A. Nytén, J.O. Thomas, Electrochem. Commun. 8 (2006) 797–800.
[10] R. Dinesh, M.K. Devaraju, T. Tomai, A. Unemoto, I. Honma, Nano Lett. 12 (2012) 1146–1151.
[11] J. Bai, Z. Gong, D. Lv, Y. Li, H. Zou, Y. Yang, J. Mater. Chem. 22 (2012) 12128–12132.
[12] Z.L. Gong, Y.X. Li, G.N. He, J. Li, Y. Yang, Electrochem. Solid-State Lett. 11 (2008) A60–A63.
[13] R. Dominko, D.E. Conte, D. Hanzel, M. Gaberscek, J. Jamnik, J. Power Sources 178 (2007) 842–847.
[14] Z. Zheng, Y. Wang, A. Zhang, T. Zhang, F. Cheng, Z. Tao, J. Chen, J. Power Sources 198 (2012) 229–235.
[15] T. Muraliganth, K.R. Stroukoff, A. Manthiram, Chem. Mater. 22 (2010) 5754–5761.
[16] C. Deng, S. Zhang, S.Y. Yang, B.L. Fu, L. Ma, J. Power Sources 196 (2011) 386–392.
[17] S. Zhang, C. Deng, B.L. Fu, S.Y. Yang, L. Ma, Electrochim. Acta 55 (2010) 8482–8489.
[18] H. Hao, J. Wang, J. Liu, T. Huang, A. Yu, J. Power Sources 210 (2012) 397–401.
[19] X.Z. Wu, X. Jiang, Q.S. Huo, Y.X. Zhang, Electrochim. Acta 80 (2012) 50–55.
[20] H. Yang, X.L. Wu, M.H. Cao, Y.G. Guo, J. Phys. Chem. C 113 (2009) 3345–3351.
[21] K. Saravanan, P. Balaya, M.V. Reddy, B.V.R. Chowdari, J.J. Vittal, Energy Environ. Sci. 3 (2010) 457–463.
[22] C. Su, L. Xu, B. Wu, C. Zhang, Electrochim. Acta 56 (2011) 10204–10209.
[23] D. Rangappa, K. Sone, T. Kudo, I. Honma, J. Power Sources 195 (2010) 6167–6171.
[24] T. Muraliganth, A.V. Murugan, A. Manthiram, J. Mater. Chem. 18 (2008) 5661–5668.
[25] Y. Zhao, J.X. Li, N. Wang, C.X. Wu, Y.H. Ding, L.H. Guan, J. Mater. Chem. 22 (2012) 18797–18800.
[26] Z.P. Yan, S. Cai, X. Zhou, Y.M. Zhao, L.J. Miao, J. Electrochem. Soc. 159 (2012) A894–A898.
[27] R. Dominko, M. Bele, M. Gaberšček, A. Meden, M. Remškar, J. Jamnik, Electrochem. Commun. 8 (2006) 217–222.
[28] B. Shao, I. Taniguchi, J. Power Sources 199 (2012) 278–286.
[29] M. Dahbi, S. Urbonaite, T. Gustafsson, J. Power Sources 205 (2012) 456–462.
[30] G. Mali, C. Sirisopanaporn, C. Masquelier, D. Hanzel, R. Dominko, Chem. Mater. 23 (2011) 2735–2744.
[31] C. Sirisopanaporn, A. Boulineau, D. Hanzel, R. Dominko, B. Budic, A.R. Armstrong, P.G. Bruce, C. Masquelier, Inorg. Chem. 49 (2010) 7446–7451.
[32] A.R. Armstrong, N. Kuganathan, M.S. Islam, P.G. Bruce, J. Am. Chem. Soc. 133 (2011) 13031–13035.
[33] F. Teng, S. Santhanagopalan, B. Asthana, X.B. Geng, S. Mho, R. Shahbazian-Yassar, D.D. Meng, J. Cryst. Growth 312 (2010) 3493–3502.
[34] A. Kojima, T. Kojima, M. Tabuchi, T. Sakai, J. Electrochem. Soc. 159 (2012) A725–A729.
[35] P.J. Zuo, T. Wang, G.Y. Cheng, X.Q. Cheng, C.Y. Du, G.P. Yin, RSC Adv. 2 (2012) 6994–6998.
[36] L. Qu, S.H. Fang, L. Yang, S. Hirano, J. Power Sources 217 (2012) 243–247.
[37] Y. Jin, C.P. Yang, X.H. Rui, T. Cheng, C.H. Chen, J. Power Sources 196 (2011) 5623–5630.
[38] A. Nytén, S. Kamali, L. Häggström, T. Gustafsson, John O. Thomas, J. Mater. Chem. 16 (2006) 2266–2272.